Research Square

Preprints are preliminary reports that have not undergone peer review.
They should not be considered conclusive, used to inform clinical practice,
or referenced by the media as validated information.

Eco-Bifunctional CuO Thin films: Tuning antibacterial and photocatalytic response via molarity adjustment molarities using spray pyrolysis

Mouad Chettab

mouad.chettab@doc.umc.edu.dz

Université de Frères Mentouri Constantine 1

Halima Djaaboube

Université de Frères Mentouri Constantine 1

Yassine Bouachiba

Ecole Nationale Polytechnique de Constantine Malek Bennabi

Safia Harrat

Constantine 01 University

Adel Taabouche

Ecole Normale Supérieure El Katiba Assia Djebar Constantine

Redha Aouati

Université de Frères Mentouri Constantine 1

Sihem Abed

Ecole Normale Supérieure El Katiba Assia Djebar Constantine

Ouidad Abdlazziz

Laboratoire de biochimie appliquée, Université des Frères Mentouri Constantine 1, Constantine, Algérie.

Research Article

Keywords: Molarity, CuO thin films, Antibacterial activity, Photocatalytic process

Posted Date: May 13th, 2026

DOI: https://doi.org/10.21203/rs.3.rs-9581586/v1

License: This work is licensed under a Creative Commons Attribution 4.0 International License.
Read Full License

Additional Declarations: No competing interests reported.

Eco-Bifunctional CuO Thin films: Tuning antibacterial and photocatalytic response via molarity adjustment molarities using spray pyrolysis.

Mouad Chettab[1*], Halima Djaaboube[1], Yassine Bouachiba[2], Safia Harrat[3] Adel Taabouche[4], Redha Aouati[1], Sihem Abed[4] and Ouidad Abdlazziz[5]

[1] Thin films and interfaces laboratory, Université de Frères Mentouri Constantine 1, Constantine, Algérie.
[2] Laboratoire Technologie des Matériaux Avancés, Ecole Nationale Polytechnique de Constantine Malek Bennabi, BP 75A RP, Ali Mendjeli, Constantine, Algérie.
[3] Laboratory of Innovative Environmental Preservation Techniques, Department of Chemistry, Constantine 01 University, 25000 Constantine, Algeria.
[4] Département de Physique et Chimie, Ecole Normale Supérieure El Katiba Assia Djebar Constantine, Constantine, Algeria.
[5] Laboratoire de biochimie appliquée, Université des Frères Mentouri Constantine 1, Constantine, Algérie.

Corresponding author: Mouad Chattab*
mouad.chettab@doc.umc.edu.dz*

Abstract

Copper oxide (CuO) thin films were successfully deposited by spray pyrolysis using precursor solutions with different molarities (0.02, 0.05 and 0.1 M) in order to investigate the correlation between growth conditions and multifunctional properties. Structural analysis confirmed the formation of monoclinic CuO with improved crystallinity as the molarity increased. The crystallite size increased to ∼17 nm while the strain and dislocation density decreased, indicating enhanced crystal quality at higher precursor concentrations. In FTIR spectra, it was observed that the bonding at 760 and 912 cm^{-1} which attributed to Cu-O stretching bonds which confirms the formation of CuO phase. Surface morphology analysis showed that higher molarity led to increased roughness and grain size to ∼ 61 nm and ∼1.9×10^5 nm respectively, reflecting a smoother and more homogeneous surface. Optical studies revealed a decrease in optical bandgap to 1.41 eV at 0.1 M. The Urbach energy increased to 0.89 eV at the same molarity indicating a low disorder and defect density in the films. Surface morphology analysis showed that higher molarity led to increased roughness and grain size to ∼ 61 nm and ∼1.9×10^5 nm respectively. Electrical measurements demonstrated a significant enhancement in conductivity with increasing molarity reaching to 7.88 x 10^{13} cm^{-3}, driven by the combined effect of higher carrier concentration and improved mobility due to reduced grain boundary scattering. Photocatalytic performance evaluated through methylene blue (MB) degradation under natural sunlight revealed that the 0.02 M film exhibited the highest degradation efficiency ~70.21 %, which is attributed to its higher surface area ~ 67.91 m^2 /g and greater density of active sites. In contrast, antibacterial activity tests showed that films prepared at higher molarity 0.1 M exhibited superior bactericidal performance, particularly against Gram-negative bacteria, due to enhanced Cu^{2+} ion release and increased generation of reactive oxygen species (ROS). These findings demonstrate a clear trade-off between photocatalytic and antibacterial performance, governed by precursor molarity. The study highlights molarity control as a simple and effective strategy for tailoring CuO thin films toward eco-friendly multifunctional applications in environmental remediation and antimicrobial coatings.

Keywords: Molarity, CuO thin films, Antibacterial activity, Photocatalytic process

1. Introduction

Copper oxide (CuO) thin films have attracted significant attention in recent years due to their remarkable physical, chemical, and biological properties, making them suitable for a wide range of technological applications [1]. As a p-type semiconductor with a narrow bandgap typically ranging from 1.2 to 2.1 eV [2], CuO exhibits excellent optical absorption in the visible region, good electrical conductivity [3], and strong chemical stability that can be tuned by varying its synthesis conditions [4]. In recent years, the development of CuO thin films with specific properties has been actively pursued for photovoltaic [5], gas sensors [6], and catalysis [7] applications. In particular, the growing demand for environmentally friendly and cost-effective solutions to address water pollution and microbial contamination has intensified research on multifunctional materials. CuO thin films have emerged as attractive candidates due to their dual capability to degrade organic pollutants through photocatalytic processes and to inhibit bacterial

growth via intrinsic antibacterial mechanisms [8,9]. These properties are mainly associated with the generation of reactive oxygen species (ROS), release of copper ions (Cu^{2+}/Cu^{+}) [9], and strong interaction with microbial cell membranes [10]. In addition to environmental pollution, the rapid emergence of antimicrobial resistance (AMR) has become a major global health concern [11]. According to the World Health Organization, bacterial infections associated with antimicrobial resistance are responsible for millions of deaths annually highlighting the urgent need for alternative antibacterial strategies that do not rely on conventional antibiotics [12]. In this context, metal oxide-based materials such as CuO have gained increasing attention due to their intrinsic antimicrobial properties [13] and their ability to generate reactive oxygen species (ROS) that effectively inactivate microorganisms [14]. The functional performance of CuO thin films is highly dependent on their structural, morphological, and electronic properties, which are strongly influenced by synthesis conditions. Among the various deposition techniques, spray pyrolysis [15] is widely recognized as a simple, low-cost [16], and scalable method that allows precise control over film characteristics by adjusting parameters such as substrate temperature, precursor concentration, and deposition rate [17]. In particular, precursor molarity plays a crucial role in determining nucleation kinetics, grain growth, defect formation, and film thickness, all of which directly impact the material performance [18].

In this context, the present work aims to systematically investigate the influence of precursor molarity (0.02, 0.05 and 0.1 M) on the structural, optical, electrical, and morphological properties of CuO thin films deposited by spray pyrolysis, and to correlate these properties with their photocatalytic and antibacterial performance. Particular attention is given to understanding the relationship between microstructure, defect density, charge transport, and surface characteristics in governing the multifunctional behavior of the films. Although several studies have investigated CuO thin films for either photocatalytic [19] or antibacterial application [11], most of them focus on complex strategies such as doping, heterostructure formation, or nanocomposite design to enhance performance. However, the effect of precursor molarity as a single, controllable parameter for tuning both functionalities simultaneously remains insufficiently explored, especially in thin film systems [20].

The originality of this work lies in demonstrating that precursor molarity alone can be used as a simple and effective parameter to tune the balance between photocatalytic and antibacterial activity. A clear trade-off is identified, where low molarity enhances photocatalytic efficiency due to higher surface area and active sites, while high molarity improves antibacterial performance through increased Cu^{2+} ion release and enhanced reactive oxygen species generation. This study provides a scalable and cost-effective approach for designing bifunctional CuO thin films for environmental and biomedical applications.

2. Experimental details and characterization techniques

In this study, CuO thin films were synthesized using spray pyrolysis at a substrate temperature of 400°C, with precursor solution molarities of 0.02, 0.05 and 0.1 M. The deposition process was meticulously controlled to ensure uniform film formation, with parameters such as the atomizer-to-substrate distance (17 cm), deposition time (10 minutes), and precursor solution composition carefully optimized less than 1 bar. This systematic approach ensures consistency in the preparation and facilitates a comprehensive investigation of the effects of molarity on the structural and functional properties of the CuO thin films. Copper acetate was employed as the precursor, while distilled water was used as the solvent to ensure environmental compatibility. The films were deposited on glass substrates, with dimensions of 2 cm x 7 cm, which had been pre-cleaned using a rigorous protocol involving methanol, acetone, and distilled water to eliminate surface contaminants, optimal film adhesion and uniformity, the protocol was illustrated in figure 01. When copper acetate is dissolved in distilled water, it dissociates into its ions. The chemical equation (i) is as follows:

$$Cu(CH_3COO)_2 + H_2O \xrightarrow{\textbf{dissociation in water}} Cu^{2+} + 2CH_3COO^- + H_2O \quad \text{(i)}$$

When solution is deposited on glass substrate at 400°C, it decomposes to form copper oxide (CuO), carbon dioxide (CO_2) and acetic acid ($2CH_3COOH$) the reaction is as follows in equation (ii):

$$Cu^{2+} + 2CH_3COO^- + H_2O \xrightarrow{\text{at } 400^\circ c} CuO + 2CO_2\uparrow + 2CH_3COOH\uparrow \quad \text{(ii)}$$

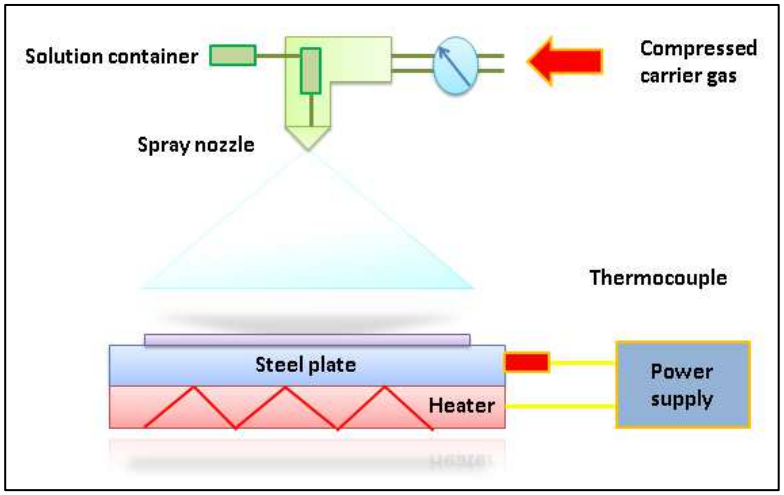


Figure 01. Illustrations for the deposition method of CuO thin films via spray pyrolysis.

3. Result and discussion

3.1 XRD results

XRD analysis were carried out to investigate the structural properties of CuO nanostructures thin films deposited on glass substrates with different molarities concentrations. The observed XRD pattern for CuO nanostructures thin films in the scan range of 25 to 70˚ are shown in figure 02. The XRD pattern of CuO contained the diffraction peaks at 2θ~32.4274, 35.9289, 38.9699, 48.9704, 53.8922, 58.3185, 61.8675, 65.9323 and 67.7934° which are assigned to reflection planes of (110), (002), (200), (-202), (020), (202), (-113), (022) and (113) show the monoclinic Tenorite structure of CuO (JCPDS card number 00-041-0254).

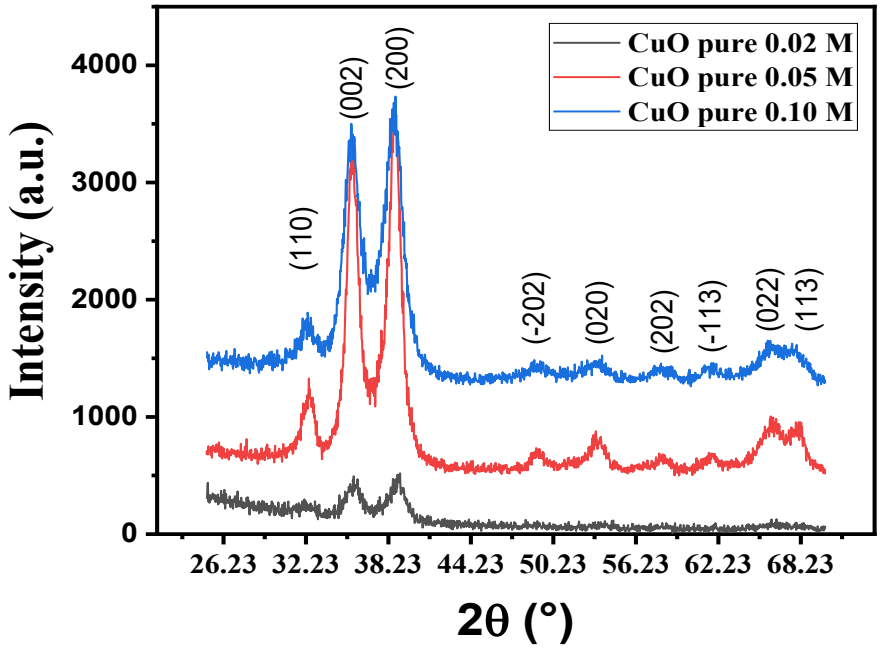


Figure 02. XRD patterns of CuO thin films with different molarities.

The lattice parameters (a, b, c and β) were calculated and tabulated in table 01, and the crystalline volume also were calculated using the equation [21]. In addition, the specific surface area SSA was calculated using the equations (2) [22, 23] and tabulated in table 01:

$$V = abc\ \sin\beta \quad (1)$$

$$SSA = \frac{6000}{D \times \gamma} \quad (2)$$

Where D and γ are the average crystalline size and the density of CuO thin films respectively. It was observed that the SSA decreased with an increase of molarity. The highest value (67.91 m^2/g) was obtained at 0.02 M, which can be the best candidate for photocatalytic test. This trend reflects the growth of larger crystallites at high molarity which reduce the surface to volume ratio, the same results were reported by Khlifi et al. [23]. The volume increases with the increasing of the molarities due to internal stress and defects formation during the deposition process. Also, the lattice parameters (a, b, c and β) were very close to the standard values in PDF card (JCPDS card number 00-041-0254).

Table 01. Variation of lattice parameters with different molarities.

Molarity (M)	a (A°)	b(A°)	c(A°)	β (°)	V ($Å^3$)	SSA (m^2/g)
0.02	4.682	3.402	5.064	98.80	79.75	67.91
0.05	4.723	3.432	5.104	98.95	81.18	54.44
0.1	4.723	3.425	5.083	99.20	81.71	52.97

To investigate the variation of crystalline size of CuO thin films; Scherrer's equation (equation 3) was utilized by measuring the full width at the half-maximum (FWHM) of the most intense diffraction peaks (002) and (200) [24].

$$D = \frac{k\lambda}{\beta_{hkl}\cos\theta} \quad (3)$$

Where k is the shape factor (k = 0,9), λ is the X-ray wavelength (λ = 1.54 Å for Cu Kα radiation), β_{hkl} is the full width at half maximum of the peak and θ is the Bragg's angle. The variation of strain and dislocation density was estimated using equations (4) and (5) [24].

$$\varepsilon = \frac{\beta_{hkl}\cos\theta}{4} \quad (4)$$

$$\delta = \frac{1}{D^2} \quad (5)$$

According to figures 03, the average crystalline size increased to ~17 nm while the strain and dislocation density decreased with the increase of molarity. This trend can be explained by nucleation growth mechanism. On the one hand, at high molarity 0.1M, the concentration of Cu^{2+} ions in solution increased where enhancing the formation of nucleation mechanism and coalescence process which contribute in the enlargement of grain size. Furthermore, more atoms were arranged closer to their equilibrium positions reducing the stress and strain in CuO lattice. This reduction can cause expansion in lattice parameters. On the other hand, at low molarity 0.02 M; less material per unit time were deposited, which can raise the grain boundaries and crystalline defects [25].

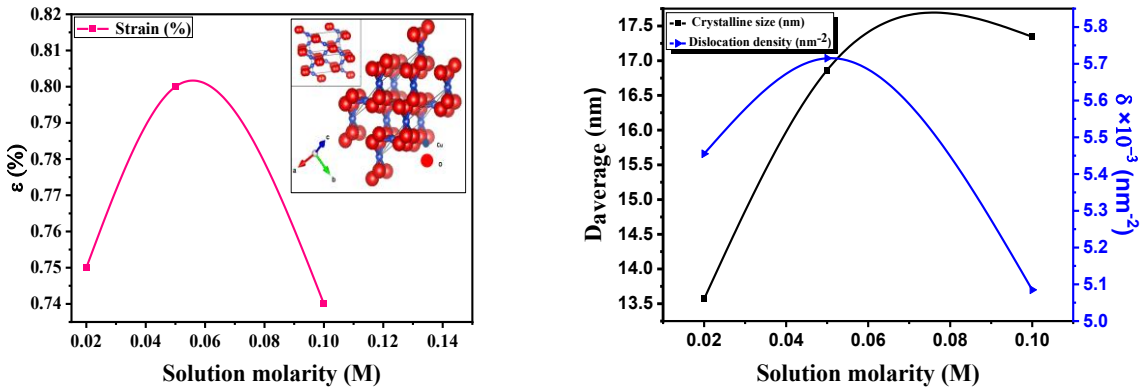


Figure 03. Variation of deformation in CuO lattice with different molarities (left). Variation of crystalline size and dislocation density with different molarities (right).

3.2 FTIR Spectroscopy

FTIR Spectroscopy was utilized to identify the Cu-O bonding and the other vibration bonds existing in CuO thin films with different molarities ranging from 400 to 4000 cm^{-1}. According to the figure 04, it was observed that the bonding at $760,912 \pm 4$ cm^{-1} which attributed to Cu-O stretching bonds [Cuo58]. The peaks that situated at 1407 and 1576 cm^{-1} were related to H-O-H bending or adsorbed water. The CO_2 peak was appeared at 2855 cm^{-1}, which came from residual of utilized precursor (copper acetate) [26]. The last peak at 2926 cm^{-1} could be attributed to O-H stretching vibrations which can enhance the antibacterial activity. The zoomed plot (400 to 1000 cm^{-1}) showed a clear shifting to higher wavenumbers which confirms our findings in XRD results. These results are in good agreement with Sone et al. [27].

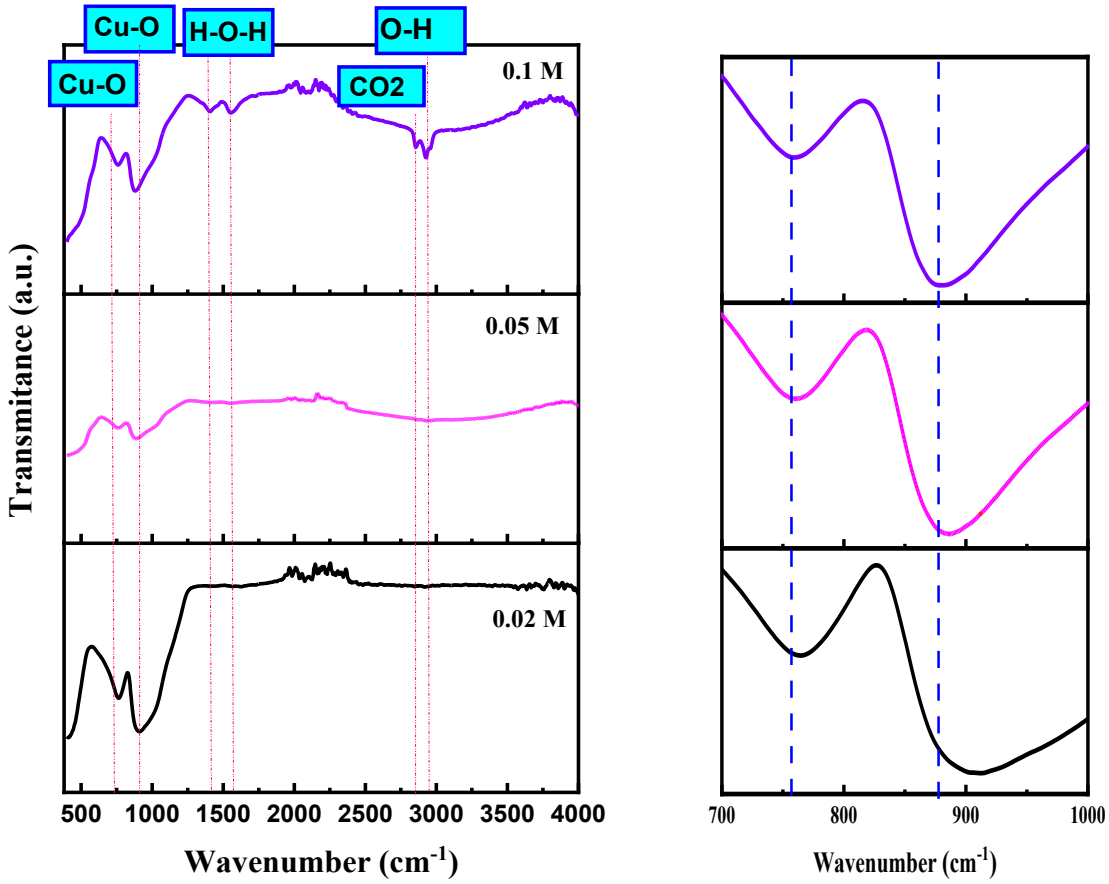


Figure 04. FTIR spectra of CuO thin films with different molarities (left), and the zoomed section (right).

3. AFM analysis

The AFM results for CuO thin films prepared with different molarities (0.02 0.05 and 0.1M) highlight clear trends in surface roughness and grain size, which are significant factors for determining the films quality and potential application including antibacterial and photocatalytical properties. According to 2D and 3D images (figure 05), the roughness increases with the solution concentration because the higher concentration result in larger droplets during spray process leading to the deposition of bigger particles and rougher films. In contrast, films prepared with lower solution concentration such as 0.02 M exhibit smoother surface because the process of deposition is more uniform. These results confirmed our findings in XRD. Figure 06 displayed that the grain size increased and the number of particles decreased with higher solution concentration to $\sim 1.9\times10^{5}$ nm and ~1200 respectively (0.1 M); larger grain sizes are associated with enhanced crystallinity and fewer grain boundaries contribute to better electrical conductivity and the stability of the films. On the other hand, the higher density of grain boundaries at lower concentration can lead to create active sites that can significantly enhance certain properties, such as antibacterial activity [28].

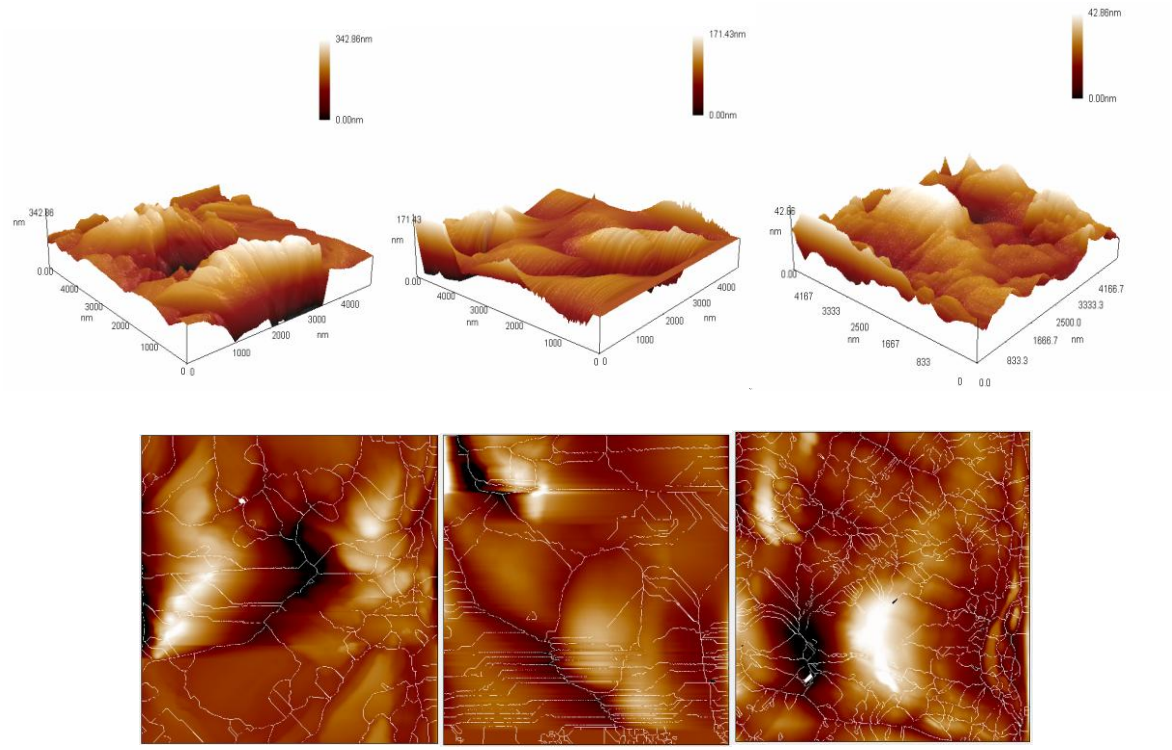


Figure 05. 2D and 3D pictures of the AFM 5×5 μm^2 area.

According to figure 07 and table 02, the surface morphology of CuO thin films shows a notable dependence on precursor molarity, as reflected in the tabulated roughness parameters. At 0.1 M, the film exhibited a relatively high average roughness (Sa = 43.1 nm) and root mean square roughness (RMS = 61 nm), indicating a rougher surface with more distinct height variations. As the molarity decreases to 0.05 and 0.2 M, both Sa and RMS decrease progressively to 17.7/24.4 nm and 5.93/5.2 nm respectively, reflecting a smoother and more homogeneous surface. The Skewness (Ssk), which indicates the symmetry of surface height distribution, shifts from a slightly positive value (0.165) at 0.02 M to negative values (0.237 at 0.05 M and 0.287 at 0.1 M), suggesting a transition from a peak-dominated to a valley-dominated surface topology, the results were reported by H. Zare Asl et al. [29]. The kurtosis (Sku), which reflects the sharpness of the height distribution, remains relatively stable across pointing to minor changes in peak sharpness. Notably, the peak-to-valley height (Sy) and the ten-point height (Sz) both increase from 42.9 nm at 0.02 M to 340 nm at 0.1 M, indicating an increasing in extreme height differences on the film surface. This confirms the formation of more sharply and rougher films at high molarities.

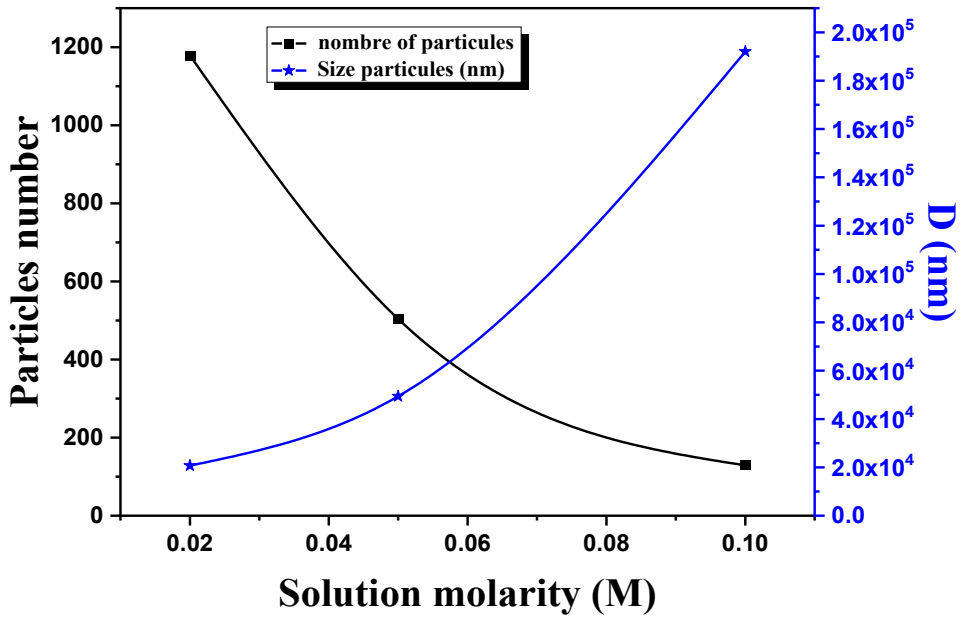


Figure 06. Particles number and particles size variations as function of solution molarity.

Table 02. Variations of high average roughness, root mean square roughness and kurtosis of CuO thin films.

Molarity (M)	0.02	0.05	0.1
Sa (nm)	5.93	17.7	43.1
RMS (nm)	17	24.4	61
Sku (nm)	3.7	4.65	3.94

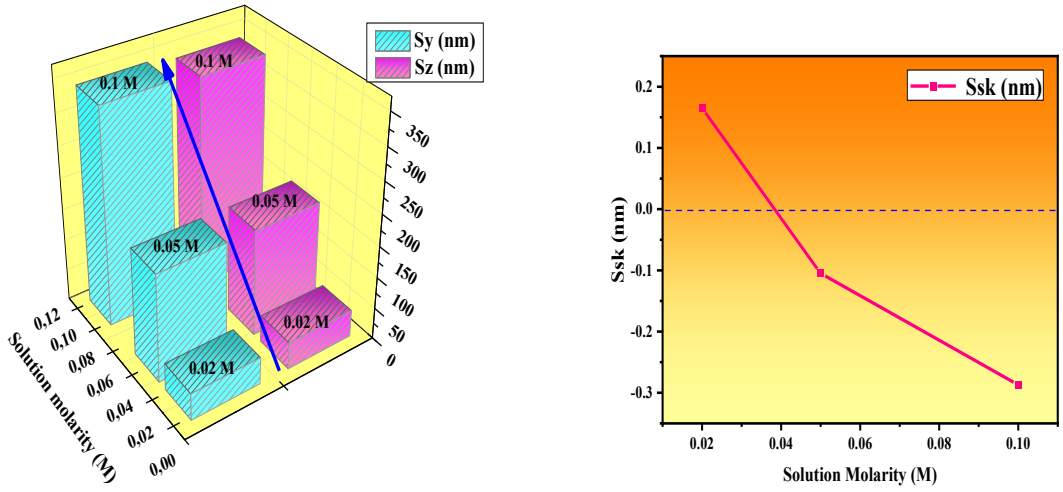


Figure 07. Peak-to-valley height (Sy) and ten-point height (Sz) (left), and Skewness variation versus molarity (right).

4. Optical properties

The transmittance behavior of CuO thin films with different molarities (0.02, 0.05 and 0.1 M) was investigated using UV-vis in the range between 400 nm to 900 nm. It was observed that the transmittance of CuO thin films decreased with the increasing of molarity, which can be explained by the elevation of the concentration of Cu^{2+} ions in the droplets in solution during the spray pyrolysis process, leading to higher deposition rate per unit time. Moreover, elevated precursor concentrations such as 0.1 M accelerated the nucleation and grain growth, yielding thicker and denser CuO films. These thicker films absorb more photons; however, this also leads to increased light scattering of films, causing reduces effective transmission as demonstrated in the accompanying figure 08. The Beer–Lambert's law ($I_T = I_0\, e^{-\alpha d}$) describes how light intensity decreases when it propagates through a thin film. When α is the absorption coefficient, d is thickness of thin films, I_0 is incident intensity light and I_T is transmitted light. There is also a correlation effect between the topological, morphological and the optical proprieties. The results obtained using AFM are providing these insights into how the surface morphology can evolve with the molarity. It is well known that the increase in the grain size could cause the red shift of absorption edge [30]. The fluctuations in zoomed section are caused by interference fringes. The CuO crystal is biaxial and optically anisotropic due to its monoclinic crystal structure, which leads to the double refraction. The double refraction in a polycrystalline film causes light scattering [31]. Similar observations have been reported in [32, 33]

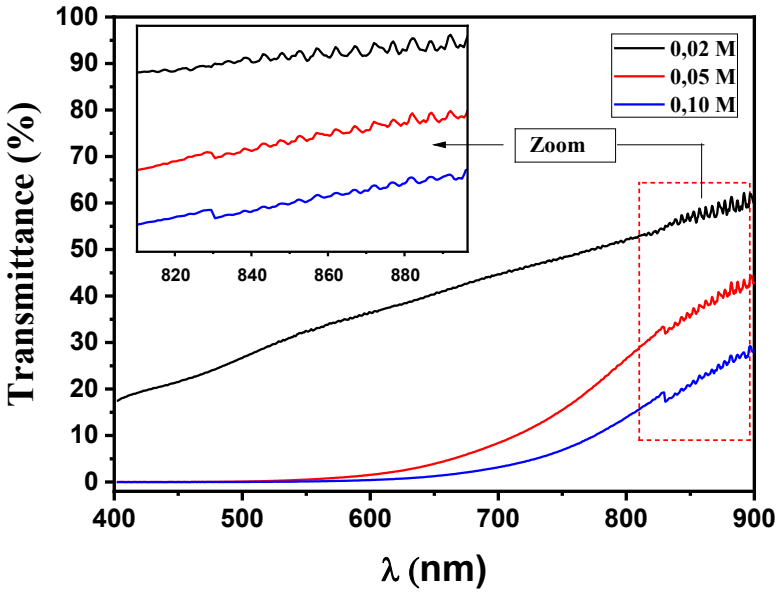


Figure 08. Transmittance spectra of CuO thin films with different molarities with zoomed section.

The Taus's equation (equation 6) was utilized to estimate the bandgap energy [15]:

$$(\alpha h\upsilon) = C(h\upsilon - Eg)^n \qquad (6)$$

Where, α is the absorption coefficient, hυ is the photon energy, Eg is the bandgap, C is a constant and the n exponent depends on the nature of electronic transition (n = 1/2 for allowed direct transition of CuO optical band). According to figure 09 the bandgap was reduced with the increasing of molarity which can be explained by the degrading of stoichiometry. Additionally, at higher precursor concentrations the oxygen vacancies V_o and interstitials sites Cu_i create mid-gap states that trap the photons and increase the absorption of light [33].

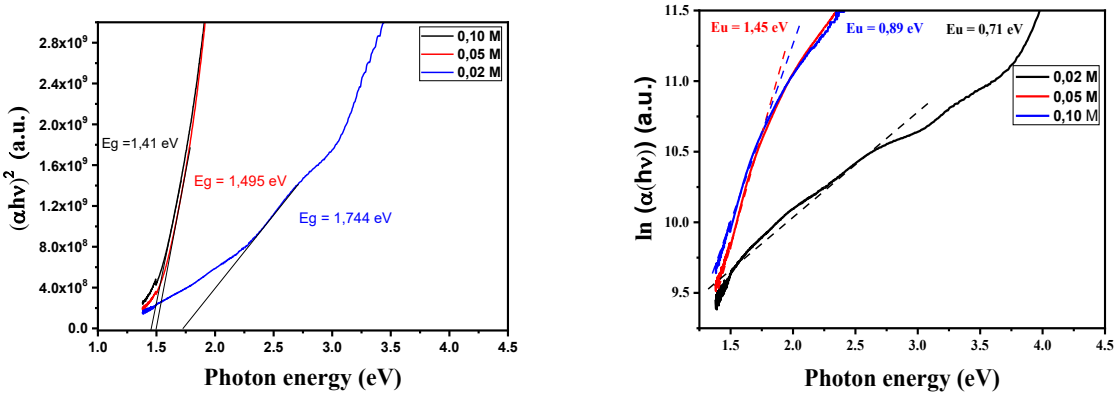


Figure 09. Tauc's plot for CuO thin films (left), Urbach energy plot for CuO thin films (right).

Equations (7) helps us to estimate the Urbach energy Eu with different molarity [15]:

$$\alpha(h\upsilon) = \alpha_0 e^{\left(\frac{h\upsilon - Eg}{Eu}\right)} \tag{7}$$

The Urbach energy is typically determined from the slope of the exponential tail of the absorption edge. It is a measure of the degree of disorder or the density of defects in the material. The decrease in Urbach energy with increasing molarity concentration may suggest a decrease in disorder or defect density in the films which can introduce localized energy states within the band gap. The obtained results show that the Urbach energy decreases with increasing precursor molarity, indicating a progressive reduction in structural disorder and defect density. These states act as trapping or recombination centers for charge carriers, and increase the risk of carrier recombination due to the presence of defect states within the narrowed band gap [29]. The figure 10 showed an inversely proportional relationship between the bandgap and the Urbach energy, which confirm our findings. This behavior can be attributed to the improvement in crystallinity at higher molarity, as confirmed by XRD analysis, where an increase in crystallite size and a decrease in strain and dislocation density were observed.

5. Electrical properties

The electrical conductivity of CuO thin films was systematically investigated using Hall Effect measurements which were utilized to evaluate key parameters, including conductivity, resistivity, free carrier concentration and mobility. The analysis provides a comprehensive understanding of the relationship between the solution molarity and the electrical transport properties of the deposited thin films. Figure 10 illustrated the variation of conductivity and resistivity as function of solution molarity. The data revealed an increase in electrical conductivity; increases by three orders of magnitude underscoring the significant impact of solution molarity of the thin films. Furthermore, the resistivity of thin films is inversely related to its electrical conductivity. This trend can be attributed to the dual effects of increased carrier concentration and enhanced mobility due to the reduced grain boundaries. Moreover, a clear correlation was observed between the solution molarity and free carrier concentration, which increased from 4.96×10^{12} to 7.88×10^{13} cm^{-3}. It is well known that; the conductivity of semiconductor it be expressed by equation (8):

$$\sigma = p \times \mu \times q \tag{8}$$

Where p is the free carrier concentration, μ is mobility and q is the elementary electronic charge. This fundamental relationship implies that the electrical conductivity is directly proportional to the product of the carriers' concentration and mobility. Consequently, any enhancement in these two parameters will improve the conductivity. Also, the mobility is intrinsically linked to the microstructure properties of the material, particularly the crystal structure. The observed relationship between crystallite size, mobility and conductivity highlighted the pivotal role of grain boundaries in determining the electrical transport behavior of CuO thin films. An increase in crystalline size generally can lead to improved mobility as larger crystallites reduce the density of grain boundaries, which are known to impede charge carrier transport [34]. The grain boundaries effect, which arises due to carrier trapping

and scattering at these interfaces. These boundaries introduce localized states within the bandage, which can capture more free carries and reduce the mobility. The trend was observed in [32, 33].

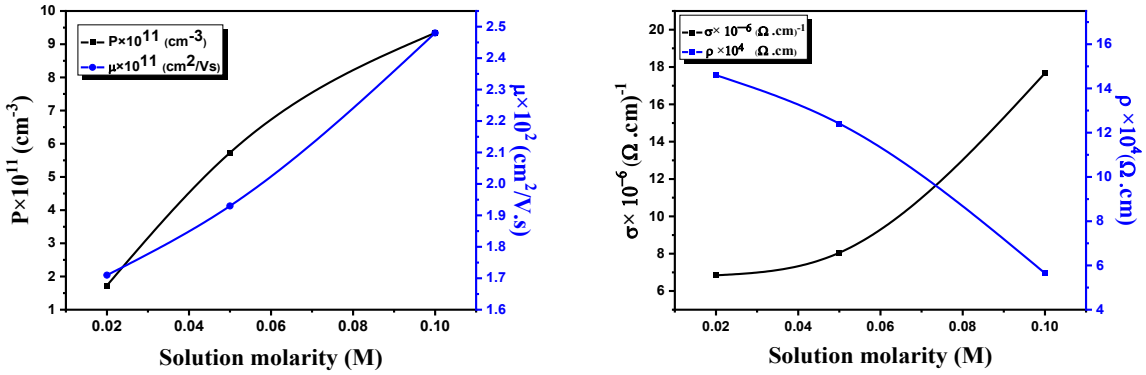


Figure 10. The mobility (μ), carrier charge density (P), the resistivity (ρ) and conductivity (σ) variation as a function of solution molarity.

6. Photocatalytic test

The photocatalytic efficiency was evaluated for CuO thin films under natural sunlight. The experiment was tested in Constantine, Algeria, on June 19th 2025, from 10:00 AM to 3:00 PM, using sunlight as the irradiation source with an average solar intensity of approximately 6.63 kW/m² /day. For each concentration, the film was dipped in 25 mL of Methylene Blue (MB) solution. Their degradation activity was monitored every hour and the spectral absorption was recorded in the wavelength range of 400-800 nm employing UV-vis spectroscopy. Figure 11 (a, b and c) shows the evolution of the absorption of MB in the presence of copper oxide thin films under sunlight irradiation. We observe an absorption peak of MB at 663 nm (maximum peak), and a gradual decrease in the absorbance intensity as a function of irradiation time until the absorbance intensity stabilizes. This confirms that the MB decomposition mechanism is at work. This mechanism is known as photo degradation. The sunlight generates electron-hole pairs that participate in oxidation-reduction reactions. The conduction band electrons reduce O_2 to form reactive oxygen species (ROS) like $\dot{O}_2$, while valence band holes oxidize water to produce hydroxyl radicals (OH radical) $\dot{O}H$, which drive pollutant degradation. The equations (9.X, X= 1, 2, 3 and 4) can describe the mechanism of photocatalytic process to degrade MB:

$$CuO + h\upsilon \rightarrow CuO(e^-_{CB} + h^+_{VB}) \quad (9.1)$$

$$CuO(e^-_{CB}) + O_2 \rightarrow CuO + \dot{O}_2 \quad (9.2)$$

$$CuO(h^+_{VB}) + H_2O \rightarrow CuO + H^+ + \dot{O}H \quad (9.3)$$

$$\dot{O}H/\dot{O}_2 + dye(MB) \rightarrow Oxidation\ decomposition \rightarrow CO_2 + H_2O \quad (9.4)$$

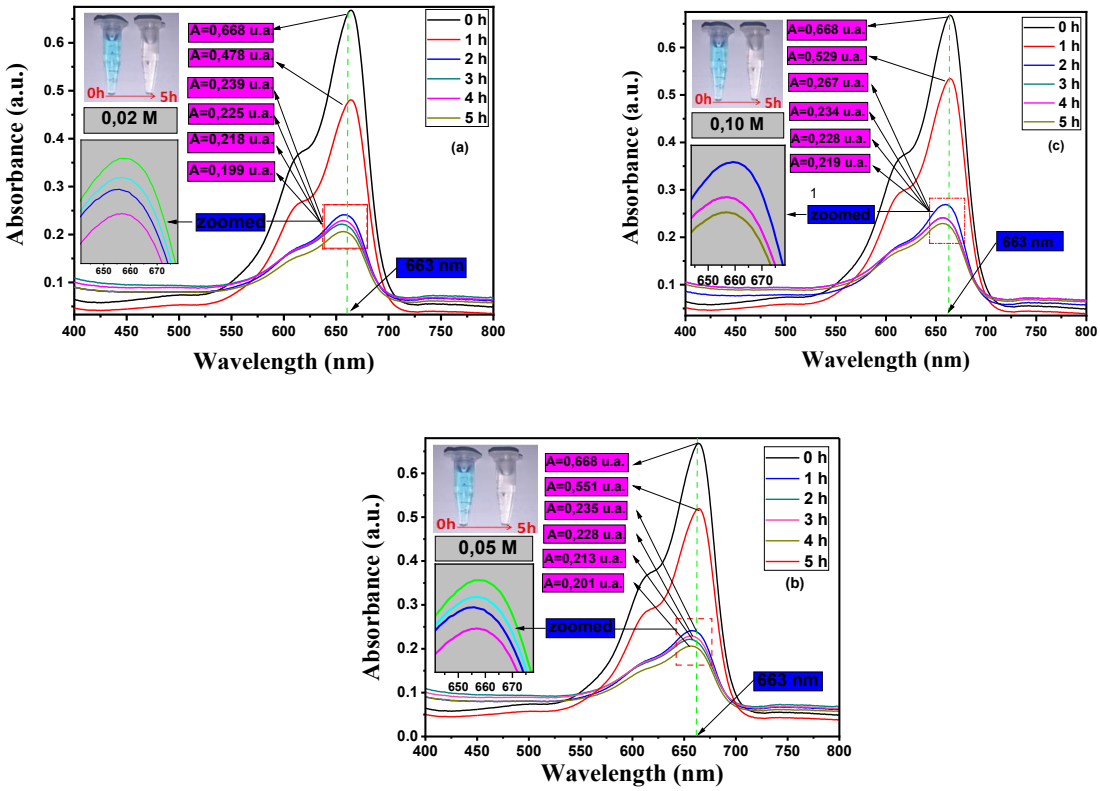


Figure 11. (a) Spectrum of MB degradation of CuO thin films at 0.02 M, (b) Spectrum of MB degradation of CuO thin films at 0.05 M, (c) Spectrum of MB degradation of CuO thin films at 0.1 M.

The equations (10) and (11) were utilized to illustrate the bandgap and different transitions between CB and VB of CuO with different molarities (0.02, 0.05 and 0.1 M) [36]:

$$E_{VB} = EA - Ee + 0.5E_g \quad (10)$$

$$E_{CB} = E_{VB} + E_g \quad (11)$$

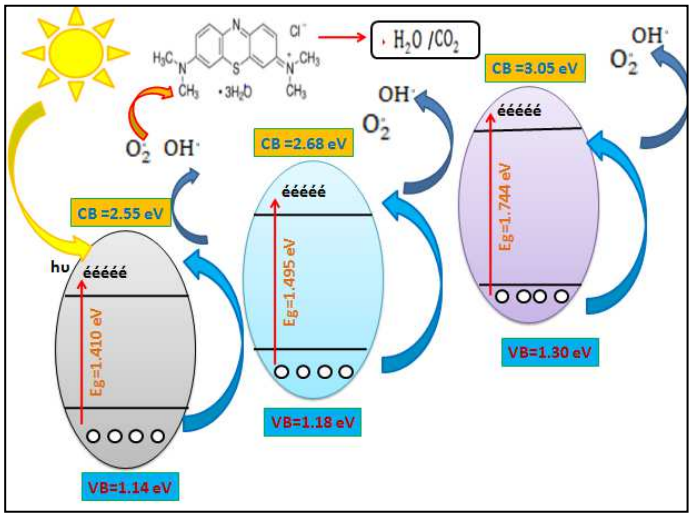


Figure 12 Illustration of electron transitions and the degradation of MB.

6.1 Degradation rate

The present study demonstrates the heterogeneity of the degradation rate as a function of the concentration of individual oxides, as visually shown in figure 13. Calculation of the degradation rate (D) according to time interval t, is carried out using formula in equation (12) [37]:

$$D = \frac{C_0 - C}{C_0} \times 100 \quad (12)$$

When, C_0 is the initial MB concentration and C is the concentration at time (t). After 5 hours of expositing in sunlight, the rate of degradation reached to 70.21, 69.91 and 67.22% for the films deposited with 0.02, 0.05 and 0.1 M respectively. According to these values of degradation rate, we can consider CuO thin films as an effective photocatalyst for MB dye. This degradation can be explained by the disorder observed at higher molarity (estimated by Urbach energy) which can influence on the motion and the velocity of charges that contribute in photocatalytic process. It is clear that the sample of 0.02 M, which has the lower Urbach energy, the degradation is higher. In addition, the high disorder in the films (0.05 M and 0.1 M) presents high defect density on surface causing saturation of photocatalytic degradation. In this case, the internal material does not participate in this process and the degradation will act slowly. Moreover, the AFM results displayed that the CuO thin films at 0.02 M exhibited a positive skewed surface which provide more reactive sites for interaction with MB while the other films showed a negative skewed surface which can influence negatively on photocatalytic process.

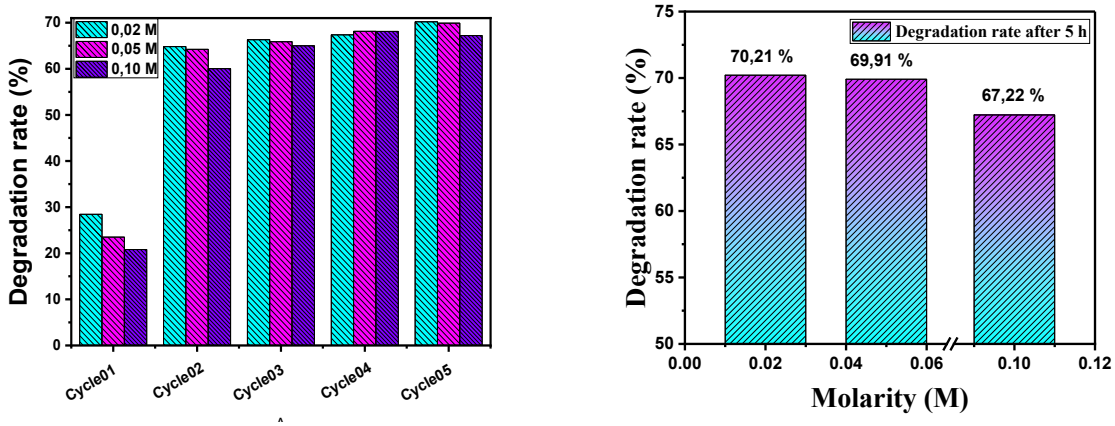


Figure 13. Photocatalytic efficiency of prepared thin films against MB dye under sunlight (left), Photocatalytic efficiency of prepared thin films against MB dye under sunlight after 5 hours (right).

6.2 Kinetic process

In photocatalytic process, the efficiency of CuO thin films depends on factors such as surface area, crystallinity, film thickness, and charge transport properties, all of which are influenced by molarity. The kinetic coefficient was estimated using the equation (13) [38]:

$$\mathrm{Ln}\left(\frac{C_t}{C_0}\right) = -kt \quad (13)$$

According to figure 14, the 0.02 M CuO film is expected to have the smallest grain size due to lower precursor concentration, leading to a relatively high surface area and a more porous structure may cause more generated $\dot{O}_2$, enhancing its photocatalytic efficiency with $k = 1.02 \times 10^{-3}\ \mathrm{min}^{-1}$. Secondly, the 0.1 M CuO film, with higher precursor concentration, results in a thicker structure and larger grains, enhancing crystallinity and reducing defect states. While it improves charge transport, its reduced surface-to-volume ratio may limit the availability of active sites, thus lowering photocatalytic efficiency ($k = 0.89 \times 10^{-3}\ \mathrm{min}^{-1}$) despite good charge mobility. The 0.05 M CuO film strikes a balance between crystallinity, charge transport, and surface area. Its moderate grain size and thickness provide sufficient active sites while maintaining good charge separation. In a methylene blue (MB) degradation experiment under sunlight with$k = 0.91 \times 10^{-3}\ \mathrm{min}^{-1}$, the 0.02 M CuO films degrade MB the fastest due to its optimal charge separation and

sufficient active sites. The 0.05 M film may show moderate degradation but suffer from charge recombination, while the 0.1 M film may degrade MB at a slower rate due to its limited surface area. Similarly, in a hydrogen evolution reaction (HER) experiment, the 0.02 M film is expected to generate the highest photocurrent and hydrogen production rate, outperforming the 0.05 M and 0.1 M films due to its well-balanced properties.

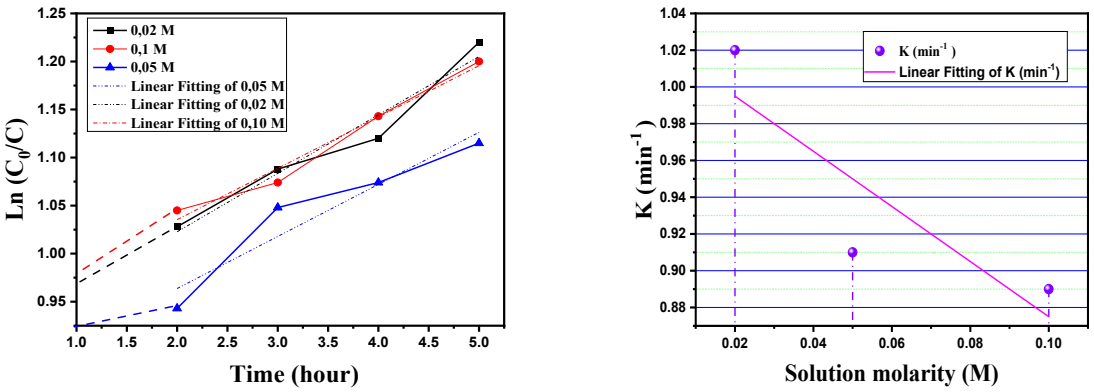


Figure 14. Plot of Ln (C_0/C) versus irradiation time for MB dye (left), variation of kinetic constant as function of CuO molarity (right).

6.3 Comparative study

To evaluate our findings with the previous studies, the degradation rate (%) of MB employing CuO thin films with different molarities was compared in table 03 which showed attractive results about the efficiency and response of our thin films toward the MB. In the upcoming studies, we will focus on complex strategies such as doping, co-doping, heterostructure formation, or nanocomposite design to enhance the photocatalytic process.

Table 03. Comparative table with the previous studies**.**

Material	Source light	Degradation rate (%)	dye	reference
ZnO:NPs	UV	46	MB	[39]
ZnO-Cu_xO	Vis	73.5	RhB	[40]
CuO/Co3O4:NPs	UV	56	MB	[41]
CuO:NPs	UV	46	MB	[41]
CuO:NPs	UV	23.4	MB	[42]
CuO (0.02M):TF	sunlight	70.21	MB	This work

TF: thin films
NPs: nanoparticles

7. Antibacterial activity

The antibacterial activity test using CuO thin films with different molarities (0.02, 0.05 and 0.1M) was investigated against E.coli: NCTC 10.538, Bacillus Spizizenii: ATCC 6633, Pseudomonas aeruginosa: NCIMB 8626 and Staph.Aureus: ATCC 6538. All the bacteria were incubated at 37 C° for 24 hour. The table 04 and figure 15 displayed the response and sensitivity of the thin films against all tested bacteria. First, E.colis exhibited a zone of inhibition (ZOI) with diameter 20, 10 and 17.5 mm for 0.1 M, 0.05 M 0.02 M respectively. A similar trend was observed for Pseudomonas aeruginosa with a maximum (ZOI) of 30 mm for 0.1 M. While Staph.Aureus and Bacillus Spizizenii showed a modest change with a peak also for 0.1 M. Our findings revealed that the CuO thin films are very sensitive to Gram negative. In contrast, Gram positive showed minimal or reduced sensitivity which is attributed to their thicker cell-wall structure [41,42].

Table 04. The Zone of inhibition (ZOI) with different molarities and Gentamicin effect for the four bacteria.

	ZOI (± 2 mm) / Molarity (M)			
Bacteria	0.1 M	0.05 M	0.02 M	Gentamicin
E.colis	20	10	17.5	35
Staph.Aureus	22.5	13	17	54
Bacillus Spizizenii	20	16	16	39
Pseudomonas aeruginosa	30	15	14.5	45

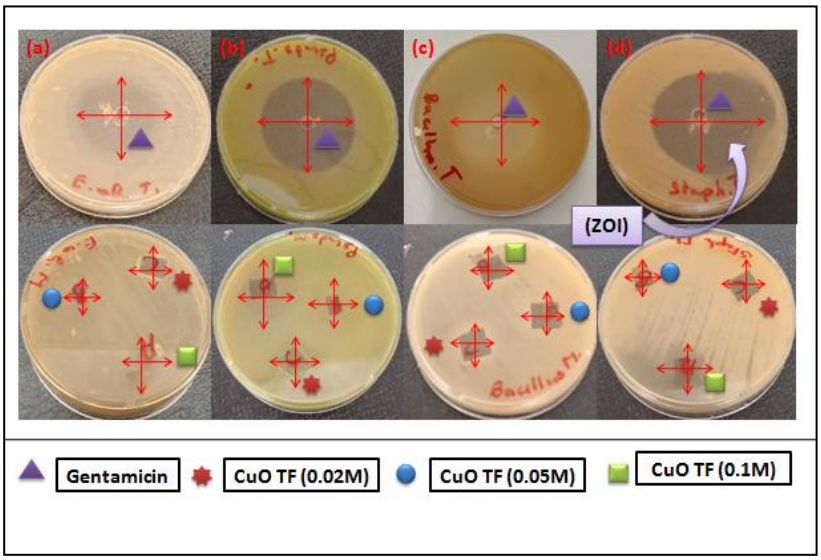


Figure 15 Images of zone of inhibition (ZOI) with different molarities and Gentamicin effect for the four bacteria.

Figure 16 showed the variations of percent kill rate for each bacterium with different molarities of CuO thin films. It is clear that all bacteria showed a high respond with CuO thin films with 0.1 M molarity where the highest value was obtained for Pseudomonas aeruginosa (66.67 %). This can be attributed to high copper content in thin films which can produce more Cu^{2+} cations release into bacterial environment. These cations increase the transport electron at the surface which leads to higher ROS production [44]. Moreover, the Surface Plasmon Resonance SPR which plays an interesting factor in antibacterial test [45]. When the CuO can respond to light, by creating a strong electromagnetic field at their surface [46].This SPR effect helps the producing of ROS and making the films more powerful in killing bacteria. Also, the AFM results revealed that the films with the high molarity (0.1 M) showed a large particles size with few numbers which reduce grain boundaries and the trapping of transfer electrons. Furthermore, the CuO thin films that prepared at 0.1 M showed a narrow bandgap which absorb more photons, leading to greater excitation of electrons from the valence band to conduction band. These e^-/h^+ participate in redox reaction that generate the ROS which can damage cell membranes [47], protein then the blocking DNA replication [48], especially through mismatched base (G-C to G-A or T-A to T-C) [49] as shown in figure 17, this oxidative damage can lead to decreasing in ATP production, which is vital energy for the cells. All the previous effects can result in cellular leakage and cell death [50].

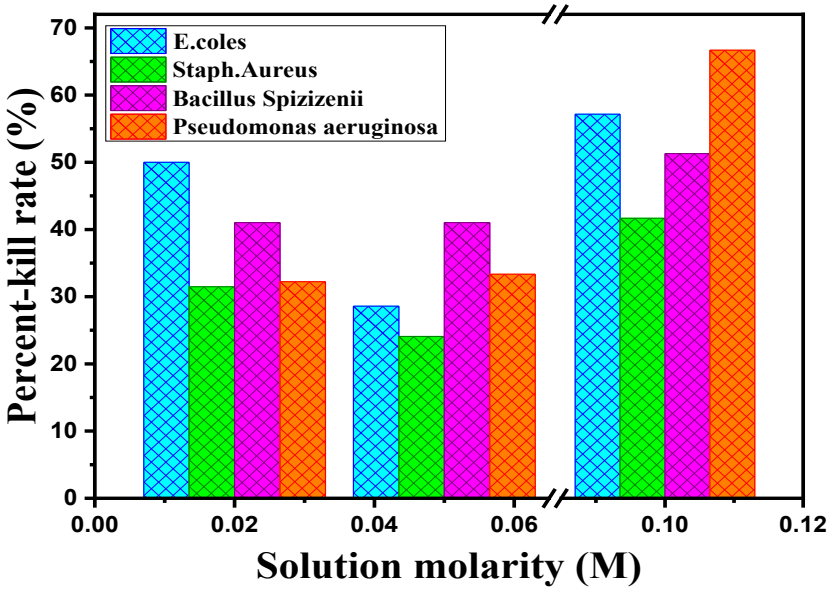


Figure 16. The percent-kill rates with different molarities for the four bacteria.

After 48 hours of incubation at 37 C°, it was observed a significant enhancement in antibacterial activity of CuO thin films. These films achieved an impressive kill rate rising to 77.78% and ZOI of 35 mm against Pseudomonas aeruginosa, practically at 0.1 M. In addition, no noticeable changes were observed for the others samples showed a little to no improvement under the same conditions. This enhancement can be explained by multiple factors. Firstly, the continuity of generation of reactive oxygen species ROS because the high molarity can product more Cu^{2+} in thin films. Secondly, the natural resistance mechanism of Pseudomonas aeruginosa also can lead to delayed and effective cell death. The positive charge induces electrostatic attraction between CuO thin films and the microorganisms' negatively charged cell membranes, allowing Cu^{2+} and Cu^{+} to adhere to cell membranes more easily causes the uncontrolled flow of components into and out of the cell. It clear that the high carrier charge density and the high mobility can improve the percent kill rates by the increasing the capacity of ions penetration (Cu^{2+} and Cu^{+}) in bacteria cell and producing damages [23].

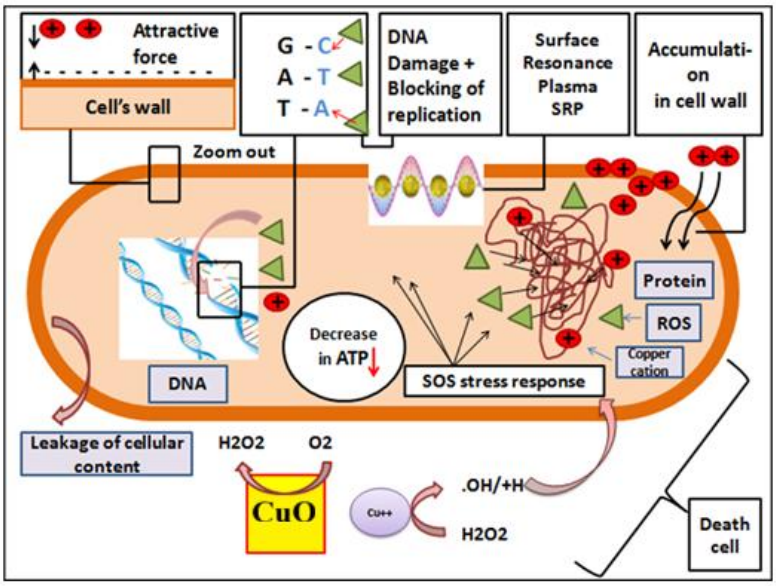


Figure 17. Illustration of antibacterial activity mechanism for CuO thin films

Conclusion

In conclusion, copper oxide (CuO) thin films were successfully deposited via spray pyrolysis, demonstrating that precursor molarity (0.02, 0.05, and 0.1 M) is a key parameter governing their structural, optoelectronic, and functional properties. Increasing molarity led to a progressive improvement in crystallinity, with crystallite size reaching ~17 nm, accompanied by a reduction in lattice strain and dislocation density, as confirmed by XRD analysis. FTIR results further validated the formation of the monoclinic CuO phase through characteristic Cu–O vibrational modes at 760 and 912 cm^{-1}. Morphological analysis revealed that higher molarity promotes grain coalescence, resulting in increased surface roughness (~61 nm) and the formation of a dense and homogeneous microstructure. Optical investigations indicated a bandgap narrowing to 1.41 eV at 0.1 M, along with a decrease in Urbach energy to 0.89 eV, suggesting reduced structural disorder and defect density. Electrical characterization supported these findings, with carrier concentration reaching 7.88×10^{13} cm^{-3} at higher molarity, attributed to enhanced charge transport and reduced grain boundary scattering in improved crystalline networks. From a functional standpoint, photocatalytic performance under natural sunlight highlights the importance of surface characteristics in environmental remediation. The highest degradation efficiency (~70.21%) observed for the 0.02 M film is directly linked to its large specific surface area (~ 67.91 m^2/g) and high density of active sites, which favor adsorption and interfacial redox reactions. This makes low-molarity films particularly suitable for solar-driven wastewater treatment applications. In contrast, antibacterial performance is significantly enhanced in films prepared at 0.1 M, especially against Gram-negative bacteria. This behavior is attributed to controlled Cu^{2+} ion release and efficient generation of reactive oxygen species (ROS), facilitated by the dense and well-crystallized structure. Such characteristics enable prolonged antimicrobial activity and improved durability, addressing critical challenges related to surface contamination and antibiotic-resistant microorganisms. Overall, a clear trade-off emerges between photocatalytic activity and antibacterial efficiency: nanostructured, high-surface-area films favor photocatalysis, whereas highly crystalline and dense films enhance antibacterial performance. This structure–property–function relationship confirms that precursor molarity is a simple, scalable, and powerful tool for tailoring CuO thin films toward specific applications, ranging from solar-assisted environmental remediation to advanced antimicrobial coatings for healthcare and public infrastructure.

References

[1] LRPCSI, University 20 Août 1955-Skikda, P.B. 26, Route d'El-Hadaiek, 21000, Skikda, Algeria, R. Daira, B. Boudjema, Laboratory of Materials Physics and its Applications, University of M'sila, 28000 M'sila, Algeria, A. Mohammedi, and Faculty of Sciences, University of M'sila, 28009 M'sila, Algeria, "Structural, optical and electrical properties of CuO thin films deposited by spray pyrolysis technique: influence annealing process," *CL*, vol. 20, no. 4, pp. 277–284, Apr. 2023, doi: 10.15251/CL.2023.204.277.

[2] R. Daira, B. Boudjema, M. Bououdina, M. S. Aida, and C.-D. Constantinescu, "Influence of Al Doping on the Physical Properties of CuO Thin Films," *Applied Sciences*, vol. 13, no. 14, p. 8193, Jul. 2023, doi: 10.3390/app13148193.

[3] M. M. Ram, R. Thundiyil, Anusha, A. Ani, P. Poornesh, and A. Rao, "Engineering the nonlinear optical and electrical properties of Sn-doped CuO thin films via controlled doping," *J Mater Sci: Mater Electron*, vol. 36, no. 24, p. 1489, Aug. 2025, doi: 10.1007/s10854-025-15569-2.

[4] O. Ben Messaoud *et al.*, "Optoelectronic and Dielectric Properties of Tenorite CuO Thin Films Sprayed at Various Molar Concentrations," *Period. Polytech. Chem. Eng.*, vol. 68, no. 1, pp. 93–105, Mar. 2024, doi: 10.3311/PPch.22136.

[5] S. Siyalo, H. F. Etefa, and F. B. Dejene, "Enhancing structural and optical properties of CuO thin films through gallium doping: A pathway to enhanced photoluminescence and predict for solar cells applications," *Chemical Physics Impact*, vol. 10, p. 100832, Jun. 2025, doi: 10.1016/j.chphi.2025.100832.

[6] E. Arulkumar, S. Thanikaikarasan, S. Rajkumar, and W. Wondimu, “Influence of solution pH dependency on structure, optical with photoelectrochemical characteristics of SILAR deposited copper oxide thin films,” *Heliyon*, vol. 10, no. 13, p. e33579, Jul. 2024, doi: 10.1016/j.heliyon.2024.e33579.

[7] J. Liu *et al.*, “Tailoring CuO nanostructures for enhanced photocatalytic property,” *Journal of Colloid and Interface Science*, vol. 384, no. 1, pp. 1–9, Oct. 2012, doi: 10.1016/j.jcis.2012.06.044.

[8] T. Khairy *et al.*, “Antibacterial activity of green synthesized copper oxide nanoparticles against multidrug-resistant bacteria,” *Sci Rep*, vol. 14, no. 1, p. 25020, Oct. 2024, doi: 10.1038/s41598-024-75147-0.

[9] S. Meghana, P. Kabra, S. Chakraborty, and N. Padmavathy, “Understanding the pathway of antibacterial activity of copper oxide nanoparticles,” *RSC Adv.*, vol. 5, no. 16, pp. 12293–12299, 2015, doi: 10.1039/C4RA12163E.

[10] A. H. Hashem *et al.*, “Synthesis and characterization of innovative GA@Ag-CuO nanocomposite with potent antimicrobial and anticancer properties,” *Sci Rep*, vol. 15, no. 1, p. 689, Jan. 2025, doi: 10.1038/s41598-024-76446-2.

[11] Md. A. Salam *et al.*, “Antimicrobial Resistance: A Growing Serious Threat for Global Public Health,” *Healthcare*, vol. 11, no. 13, p. 1946, Jul. 2023, doi: 10.3390/healthcare11131946.

[12] S. Sethi and T. F. Murphy, “Bacterial Infection in Chronic Obstructive Pulmonary Disease in 2000: a State-of-the-Art Review,” *Clin Microbiol Rev*, vol. 14, no. 2, pp. 336–363, Apr. 2001, doi: 10.1128/CMR.14.2.336-363.2001.

[13] S. S. Salem, A. Yousef, E. S. Abd El Hamid, S. Ibrahim, and R. H. Elbawab, “Evaluation of eco-friendly copper oxide nanoparticles for anticancer activity and antibacterial effects against Streptococcus mutans using molecular docking,” *Sci Rep*, vol. 15, no. 1, p. 40921, Nov. 2025, doi: 10.1038/s41598-025-23947-3.

[14] Z. Martínez-Corona *et al.*, “Antibacterial activity of TiO2, CuO, and CuO/TiO2 nanomaterials and their potential application on construction surfaces,” *J Mater. Sci: Mater Eng.*, vol. 20, no. 1, p. 70, May 2025, doi: 10.1186/s40712-025-00288-7.

[15] H. Djaaboube *et al.*, “Optical properties and complex refractive index of Co doped ZnO waveguide thin films elaborated by spray pyrolysis,” Apr. 01, 2022. doi: 10.21203/rs.3.rs-1513013/v1.

[16] B. Gharbi *et al.*, “Spray Pyrolysis Synthesized and ZnO–NiO Nanostructured Thin Films Analysis with Their Nanocomposites for Waveguiding Applications,” *Semiconductors*, vol. 55, no. 1, pp. 37–43, Jan. 2021, doi: 10.1134/S1063782621010085.

[17] I. Salah, E. Allan, S. P. Nair, and I. P. Parkin, “Antibacterial performance of a copper nanoparticle thin film,” *Nano Select*, vol. 5, no. 9, p. 2300134, Sep. 2024, doi: 10.1002/nano.202300134.

[18] V. Jagadeesan and V. Subramaniam, “Impact of molarity on structural, optical, morphological and electrical properties of copper oxide thin films prepared by cost effective jet nebulizer spray pyrolysis technique,” *J Mater Sci: Mater Electron*, vol. 30, no. 2, pp. 1571–1578, Jan. 2019, doi: 10.1007/s10854-018-0428-8.

[19] R. Aouati *et al.*, “Al3+ doping effect on the properties of SnO2 thin films prepared by sol-gel and dip-coating method for photocatalytic application,” *Physica B: Condensed Matter*, vol. 723, p. 418089, Feb. 2026, doi: 10.1016/j.physb.2025.418089.

[20] A. A. Akl, S. A. Mahmoud, S. M. AL-Shomar, and A. S. Hassanien, “Improving microstructural properties and minimizing crystal imperfections of nanocrystalline Cu 2 O thin films of different solution molarities for solar cell applications,” *Materials Science in Semiconductor Processing*, vol. 74, pp. 183–192, Feb. 2018, doi: 10.1016/j.mssp.2017.10.007.

[21] S. Aroussi, M. A. Dahamni, M. Ghamnia, D. Tonneau, and C. Fauquet, “Characterization of Some Physical and Photocatalytic Properties of CuO Nanofilms Synthesized by a Gentle Chemical Technique,” *Condensed Matter*, vol. 7, no. 2, p. 37, May 2022, doi: 10.3390/condmat7020037.

[22] C. Sahin, U. Arabaci, D. T. Bulut, and P. Obakan Yerlikaya, “Synthesis and Characterization of Ag Doped CuO Nanoparticles with Different Sizes and Investigation of Their Anticancer Activity,” *J Inorg Organomet Polym*, vol. 35, no. 11, pp. 8889–8902, Nov. 2025, doi: 10.1007/s10904-025-03799-0.

[23] N. Khlifi *et al.*, “Non-doped and transition metal-doped CuO nano-powders: structure-physical properties and anti-adhesion activity relationship,” *RSC Adv.*, vol. 12, no. 36, pp. 23527–23543, 2022, doi: 10.1039/D2RA02433K.

[24] C. Sahin, U. Arabaci, D. T. Bulut, and P. Obakan Yerlikaya, “Synthesis and Characterization of Ag Doped CuO Nanoparticles with Different Sizes and Investigation of Their Anticancer Activity,” *J Inorg Organomet Polym*, vol. 35, no. 11, pp. 8889–8902, Nov. 2025, doi: 10.1007/s10904-025-03799-0.

[25] S. Kose, F. Atay, V. Bilgin, and I. Akyuz, “Some physical properties of copper oxide films: The effect of substrate temperature,” *Materials Chemistry and Physics*, vol. 111, no. 2–3, pp. 351–358, Oct. 2008, doi: 10.1016/j.matchemphys.2008.04.025.

[26] D. Tabli, N. Touka, K. Baddari, and N. Selmi, “Pb-Doped CuO Thin Films Synthetized by Sol-Gel Method,” *Advances in Materials Science*, vol. 22, no. 3, pp. 5–13, Sep. 2022, doi: 10.2478/adms-2022-0009.

[27] B. T. Sone, A. Diallo, X. G. Fuku, A. Gurib-Fakim, and M. Maaza, “Biosynthesized CuO nano-platelets: Physical properties & enhanced thermal conductivity nanofluidics,” *Arabian Journal of Chemistry*, vol. 13, no. 1, pp. 160–170, Jan. 2020, doi: 10.1016/j.arabjc.2017.03.004.

[28] D. Das, B. C. Nath, P. Phukon, and S. K. Dolui, “Synthesis and evaluation of antioxidant and antibacterial behavior of CuO nanoparticles,” *Colloids and Surfaces B: Biointerfaces*, vol. 101, pp. 430–433, Jan. 2013, doi: 10.1016/j.colsurfb.2012.07.002.

[29] H. Zare Asl and S. Mohammad Rozati, “Spray Deposited Nanostructured CuO Thin Films: Influence of Substrate Temperature and Annealing Process,” *Mat. Res.*, vol. 21, no. 2, Jan. 2018, doi: 10.1590/1980-5373-mr-2017-0754.

[30] F. A. Akgul, G. Akgul, N. Yildirim, H. E. Unalan, and R. Turan, “Influence of thermal annealing on microstructural, morphological, optical properties and surface electronic structure of copper oxide thin films,” *Materials Chemistry and Physics*, vol. 147, no. 3, pp. 987–995, Oct. 2014, doi: 10.1016/j.matchemphys.2014.06.047.

[31] S. Kose, F. Atay, V. Bilgin, and I. Akyuz, “Some physical properties of copper oxide films: The effect of substrate temperature,” *Materials Chemistry and Physics*, vol. 111, no. 2–3, pp. 351–358, Oct. 2008, doi: 10.1016/j.matchemphys.2008.04.025.

[32] S. K. Abdo and J. M. Rzaij, “Copper Molarity Effect on the Optical Properties of Cu2CdSnS4 Quaternary Thin Films,” *eijs*, pp. 1513–1523, May 2021, doi: 10.24996/ijs.2021.62.5.15.

[33] N. Allouche *et al.*, “Morphological and optical characterization of spin-coated CuO nanostructured thin films doped with V, Na, Ba, and Er for enhanced CO2 sensing,” *Journal of Materials Research and Technology*, vol. 35, pp. 379–391, Mar. 2025, doi: 10.1016/j.jmrt.2025.01.048.

[34] D. S. Murali, S. Kumar, R. J. Choudhary, A. D. Wadikar, M. K. Jain, and A. Subrahmanyam, “Synthesis of Cu2O from CuO thin films: Optical and electrical properties,” *AIP Advances*, vol. 5, no. 4, p. 047143, Apr. 2015, doi: 10.1063/1.4919323.

[35] S. S. Chiad, S. F. Oboudi, G. H. Mohamed, and N. F. Habubi, “Solution molarity effect on electrical properties of SnO2 thin films,” *thin films*, 2014.

[36] S. T. Khlayboonme and W. Thowladda, “Impact of Al-doping on structural, electrical, and optical properties of sol-gel dip coated ZnO:Al thin films,” *Mater. Res. Express*, vol. 8, no. 7, p. 076402, Jul. 2021, doi: 10.1088/2053-1591/ac113d.

[37] M. Farooq *et al.*, “Phytoassisted synthesis of CuO and Ag–CuO nanocomposite, characterization, chemical sensing of ammonia, degradation of methylene blue,” *Sci Rep*, vol. 14, no. 1, p. 1618, Jan. 2024, doi: 10.1038/s41598-024-51391-2.

[38] S. Shivanna, D. Purushotham, A. Kodandaram, C. M. Nagabhushana, and A. Mavinakere Ramesh, “Microwave assisted hydrothermal synthesis of Ag2O/α-Bi2O3 heterostructures with highly enhanced photocatalysis and their environmental interest,” *Chemical Physics Impact*, vol. 6, p. 100241, Jun. 2023, doi: 10.1016/j.chphi.2023.100241.

[39] V. V. Pham, T. D. Nguyen, P. P. Ha La, and M. Thi Cao, “A comparison study of the photocatalytic activity of ZnO nanoparticles for organic contaminants degradation under low-power UV-A lamp,” *Adv. Nat. Sci: Nanosci. Nanotechnol.*, vol. 11, no. 1, p. 015005, Mar. 2020, doi: 10.1088/2043-6254/ab6163.

[40] P. Nandi and D. Das, “ZnO-Cu O heterostructure photocatalyst for efficient dye degradation,” *Journal of Physics and Chemistry of Solids*, vol. 143, p. 109463, Aug. 2020, doi: 10.1016/j.jpcs.2020.109463.

[41] R. X. Chen *et al.*, “Synthesis of CuO/Co_3 O_4 Coaxial Heterostructures for Efficient and Recycling Photodegradation,” *International Journal of Photoenergy*, vol. 2015, pp. 1–11, 2015, doi: 10.1155/2015/183468.

[42] P. Ponnarasi and G. Mahalakshmi, “Ag-doped CuO nanoparticles embedded reduced graphene oxide nanocomposite from Punica granatum peel extract and evaluation of their photocatalytic activity and antimicrobial potential,” *Chemical Physics Impact*, vol. 8, p. 100632, Jun. 2024, doi: 10.1016/j.chphi.2024.100632.

[43] H. T. Gebrie *et al.*, “Biosynthesis and characterization of copper oxide nanoparticles from Plumbago zeylanica leaf extract for antibacterial and antioxidant activities,” *Sci Rep*, vol. 15, no. 1, p. 30656, Aug. 2025, doi: 10.1038/s41598-025-10700-z.

[44] R. B. Asamoah *et al.*, "A Comparative Study of Antibacterial Activity of CuO/Ag and ZnO/Ag Nanocomposites," *Advances in Materials Science and Engineering*, vol. 2020, no. 1, p. 7814324, Jan. 2020, doi: 10.1155/2020/7814324.

[45] Y.-L. Chiang, C.-H. Lin, M.-Y. Yen, Y.-D. Su, S.-J. Chen, and H. Chen, "Innovative antimicrobial susceptibility testing method using surface plasmon resonance," *Biosensors and Bioelectronics*, vol. 24, no. 7, pp. 1905–1910, Mar. 2009, doi: 10.1016/j.bios.2008.09.020.

[46] A. T. Mosleh *et al.*, "Performance of Ag-doped CuO nanoparticles for photocatalytic activity applications: Synthesis, characterization, and antimicrobial activity," *Discover Nano*, vol. 19, no. 1, p. 166, Oct. 2024, doi: 10.1186/s11671-024-04108-3.

[47] S. S. Salem, A. Yousef, E. S. Abd El Hamid, S. Ibrahim, and R. H. Elbawab, "Evaluation of eco-friendly copper oxide nanoparticles for anticancer activity and antibacterial effects against Streptococcus mutans using molecular docking," *Sci Rep*, vol. 15, no. 1, p. 40921, Nov. 2025, doi: 10.1038/s41598-025-23947-3.

[48] A. H. Hashem *et al.*, "Synthesis and characterization of innovative GA@Ag-CuO nanocomposite with potent antimicrobial and anticancer properties," *Sci Rep*, vol. 15, no. 1, p. 689, Jan. 2025, doi: 10.1038/s41598-024-76446-2.

[49] T. Khairy *et al.*, "Antibacterial activity of green synthesized copper oxide nanoparticles against multidrug-resistant bacteria," *Sci Rep*, vol. 14, no. 1, p. 25020, Oct. 2024, doi: 10.1038/s41598-024-75147-0.

[50] M. K. Y. Soliman and S. S. Salem, "Comparative evaluation of antimicrobial, antibiofilm, antioxidant, antiviral, and antidiabetic activities of copper oxide nanoparticles biofabricated via Opuntia ficus indica," *Sci Rep*, vol. 15, no. 1, p. 24823, Jul. 2025, doi: 10.1038/s41598-025-08878-3.